Influence of dark matter on black hole scalar hair

Bartlomiej Kiczek* and Marek Rogatko†
Institute of Physics, Maria Curie-Sklodowska University, 20-031 Lublin, pl. Marii Curie-Sklodowskiej 1, Poland

(Received 13 February 2020; accepted 3 April 2020; published 14 April 2020)

Searches for *dark matter* sector field imprints on the astrophysical phenomena are one of the most active branches of the current researches. Using numerical methods, we elaborate the influence of dark matter on the emergence of black hole hair and formation of boson stars. We explore thermodynamics of different states of the system in Einstein-Maxwell-scalar dark matter theory with box boundary conditions. Finally, we find that the presence of dark sector within the system diminishes a chance of formation of scalar hair around a black hole.

DOI: 10.1103/PhysRevD.101.084035

I. INTRODUCTION

The astrophysical evidence of the illusive ingredient of our Universe, *dark matter*, is overwhelming and authorizes the galaxy rotation curves, gravitational lensing, a thread-like structure (cosmic web) on which ordinary matter accumulates [1,2]. On the contrary, the absence of the evidence of the most popular particle candidates for baryonic dark matter stipulates the necessity of diversifying experimental efforts [3]. Black holes and ultracompact horizonless objects being the ideal laboratories for dark matter studies may help us to answer the tantalizing question of how dark matter sector leaves its imprint in the physics of these objects. However, it happens that Schwarzschild black hole has a negative specific heat and it cannot be in equilibrium with thermal radiation. To overcome this difficulty, the idea of enclosing the black hole within a box was proposed [4,5]. Einstein-Maxwell systems with box boundary conditions were elaborated in [6], where it was established that the phase structure of the models was similar to AdS gravity. Inclusion of the additional scalar field to the theory in question envisages the correspondence of phase transitions in gravity in a box with s-wave holographic superconductor [7–9]. The thermodynamical studies of Einstein-Maxwell scalar systems in the asymptotically flat spacetime with reflecting boundary conditions were conducted in [10]. A certain range of parameters allows to obtain stable black hole solution, giving a way to circumvent no-hair theorem.

The next compact objects studied in our paper, from the point of view of the influence of dark matter on their physics, are boson stars. Boson stars being a self-gravitating solution of massive scalar field with a potential coupled to gauge fields and gravity [11] are widely studied in literature [12–16] for a quite long period of time.

The purpose of our paper is to examine thermodynamical properties and stability of the black holes and horizonless objects-boson stars in Einstein-Maxwell-scalar system influenced by dark matter sector and envisage the role of the dark matter in the elaborated problems.

The organization of the paper is as follows. In Sec. II, we describe the basic features of the *hidden sector* model and derived the basic equations needed in what follows. Section III is devoted to the description of the obtained numerical results. In Sec. IV, we concluded our researches.

II. MODEL

We consider the spacetime manifold with timelike boundary $\partial\mathcal{M}$, which will be referred as a box. The action for Einstein-Maxwell scalar dark matter gravity is provided by

$$S=\int_{\mathcal{M}} d^4x\sqrt{-g}\Big(R-\frac{1}{4}F_{\mu\nu}F^{\mu\nu}-\frac{\alpha}{4}B_{\mu\nu}F^{\mu\nu} -\frac{1}{4}B_{\mu\nu}B^{\mu\nu}-|D\Psi|^2-m^2|\Psi|^2\Big)-\int_{\partial\mathcal{M}} d^3x\sqrt{-\gamma}\mathcal{K}, \quad (1)$$

where $F_{\mu\nu}$ is a Maxwell field strength tensor, $B_{\mu\nu}$ is a strength tensor of a hidden sector vector boson. The complex scalar field $\Psi=\psi e^{i\theta}$, where θ denotes the phase, is coupled only to the ordinary electromagnetic field by the covariant derivative $D_\mu=\nabla_\mu-iqA_\mu$. The theoretical justifications of the model in question originate from M/string theories, where such mixing portals coupling Maxwell and auxiliary gauge fields can be encountered [17]. The hidden sectors states are charged under their own groups and interact with the *visible* sector via gravitational interactions. The realistic string compactifications establish the range of values for α between 10^{-2} and 10^{-10} [18–21]. It seems that astrophysical

*bkiczek@kft.umcs.lublin.pl
†rogat@kft.umcs.lublin.pl

observations of gamma rays of energy 511 keV [22], positron excess in galaxies [23], and muon anomalous magnetic moment [24] argue for the aforementioned idea of coupling Maxwell field with dark matter sector. Recent experiments aimed at gamma ray emissions from dwarf galaxies [25], dilatonlike coupling to photons caused by ultralight dark matter [26], oscillations of the fine structure constant [27], revisions of the constraints on *dark photon* 1987A supernova emission [28], measurements of excitation of electrons in CCD-like detector [29], as well as the examinations in e^+e^- Earth colliders [30], give us some hints for the correctness of the proposed model. They and the future planned ballon d'essai will ameliorate the mass constraints on the hidden sector particles, especially for dark photons.

The second integral denotes the Gibbons-Hawking boundary term of our box with γ metric on the three-dimensional hypersurface $(r = r_b)$, with the extrinsic curvature $\mathcal{K}$.

Varying the action (1), we get the equations of motion of the forms

$$(\nabla_\mu - iqA_\mu)(\nabla^\mu - iqA^\mu)\Psi - m^2\Psi = 0, \tag{2}$$

$$\tilde{\alpha}\nabla_\mu F^{\mu\nu} = j^\nu, \tag{3}$$

where $\tilde{\alpha} = 1 - \frac{\alpha^2}{4}$ and the current j^ν is provided by the relation

$$j^\nu = iq[\Psi^\dagger(\nabla^\nu - iqA^\nu)\Psi - \Psi(\nabla^\nu + iqA^\nu)\Psi^\dagger]. \tag{4}$$

In what follows, we use a time-independent spherically symmetric line element, with the metric coefficients being functions of r coordinate,

$$ds^2 = -g(r)h(r)dt^2 + \frac{dr^2}{g(r)} + r^2(d\theta^2 + \sin\theta^2 d\phi^2), \tag{5}$$

and the adequate components of the fields in the theory will constitute radial functions of the forms

$$A_\mu dx^\mu = \phi(r)dt, \qquad B_\mu dx^\mu = \chi(r)dt, \qquad \Psi = \Psi(r). \tag{6}$$

In general, the scalar field can have harmonic time dependence which can be absorbed by a redefinition of the gauge field function. Having this in mind it can be seen that the r component of the equations of motion for the gauge and scalar fields leads to the conclusion that $\Psi(r) = \psi(r)$. By virtue of this, the following equations of motion are provided:

$$R_{\mu\nu} - \frac{1}{2}g_{\mu\nu}R = T_{\mu\nu}, \tag{7}$$

$$\nabla_\mu\nabla^\mu\psi - q^2A_\mu A^\mu\psi - m^2\psi = 0, \tag{8}$$

$$\nabla_\mu F^{\mu\nu} + \frac{\alpha}{2}\nabla_\mu B^{\mu\nu} - 2q^2A^\nu\psi^2 = 0, \tag{9}$$

$$\nabla_\mu B^{\mu\nu} + \frac{\alpha}{2}\nabla_\mu F^{\mu\nu} = 0. \tag{10}$$

As in the case of Eq. (3), the last two equations can be rewritten as

$$\tilde{\alpha}\nabla_\mu F^{\mu\nu} - 2q^2A^\nu\psi^2 = 0, \tag{11}$$

$$\nabla_\mu B^{\mu\nu} + \frac{\alpha}{\tilde{\alpha}}q^2A^\nu\psi^2 = 0. \tag{12}$$

Consequently, the explicit forms of the equations of motion yield

$$h' - rh\psi'^2 - \frac{q^2r\phi^2\psi^2}{g^2} = 0, \tag{13}$$

$$g' + g\left(\frac{1}{r} + \frac{1}{2}r\psi'^2\right) + \frac{q^2r\phi^2\psi^2}{2gh} - \frac{1}{r} + \frac{r}{2h}(\phi'^2 + \alpha\chi'\phi' + \chi'^2 + m^2h\psi^2) = 0, \tag{14}$$

$$\phi'' + \left(\frac{2}{r} - \frac{h'}{2h}\right)\phi' - \frac{2q^2\phi\psi^2}{\tilde{\alpha}g} = 0, \tag{15}$$

$$\psi'' + \left(\frac{2}{r} + \frac{h'}{2h} + \frac{g'}{g}\right)\psi' + \left(\frac{q^2\phi^2}{gh} - m^2\right)\frac{\psi}{g} = 0, \tag{16}$$

$$\chi'' + \left(\frac{2}{r} - \frac{h'}{2h}\right)\chi' + \frac{\alpha q^2\chi\psi^2}{\tilde{\alpha}g} = 0. \tag{17}$$

To solve the equations of the theory in question, one has to provide adequate boundary conditions. Namely, we can pick either a horizonless or a black hole solution. In case of a black hole, we expand the underlying functions in a Taylor series around the horizon of radius r_h,

$$\psi = \psi_0 + \psi_1(r - r_h) + \psi_2(r - r_h)^2 + \mathcal{O}(r^3), \tag{18}$$

$$\phi = \phi_1(r - r_h) + \phi_2(r - r_h)^2 + \mathcal{O}(r^3), \tag{19}$$

$$g = g_1(r - r_h) + g_2(r - r_h)^2 + \mathcal{O}(r^3), \tag{20}$$

$$h = 1 + h_1(r - r_h) + \mathcal{O}(r^2), \tag{21}$$

$$\chi = \chi_1(r - r_h) + \chi_2(r - r_h)^2 + \mathcal{O}(r^3). \tag{22}$$

We set $g_0 = 0$ due to occurrence of the black hole event horizon. For the regularity of the $U(1)$-gauge fields on the event horizon, one also puts ϕ_0 and χ_0 equal to zero (in order to keep the terms with division by $g(r_h)$ in equations of motion finite). By implementing the expansions

(18)–(22) into the equations of motion, we find out that $\{r_h, \psi_0, \phi_1, \chi_1, \alpha\}$ comprise free parameters of the theory in question, while the remaining ones can be expressed by them.

As far as the boson star scenario is concerned, we perform a similar expansion. However, since the configuration in question is horizonless, the expansion accomplishes around the origin of the reference frame. At $r = 0$, we require that the derivatives of all the functions are set equal to zero, which ensures that there is no kink at this point. At $r = r_b$, we establish the Dirichlet boundary condition for the scalar field $\psi(r_b) = 0$ (the reflecting mirrorlike boundary conditions).

Asymptotic analysis of matter fields, at the box boundary, enables us to write

$$\psi \sim \psi^{(0)} + \psi^{(1)}(r_b - r) + \mathcal{O}(r^2), \tag{23}$$

$$\phi \sim \phi^{(0)} + \phi^{(1)}(r_b - r) + \mathcal{O}(r^2), \tag{24}$$

$$\chi \sim \chi^{(0)} + \chi^{(1)}(r_b - r) + \mathcal{O}(r^2). \tag{25}$$

As was proposed in Refs. [10,16], because of the fact that the scalar field satisfies the reflecting mirrorlike boundary conditions $\psi(r_b) = 0$, one can fix $\psi^{(0)} = 0$ and the other parameter $\psi^{(1)}$ can be used for the phase transition description. This approach to the problem in question is widely exploited in holographic studies of superconductors and superfluids.

For the gauge fields, one has that $\phi^{(0)} = \mu$ and $\chi^{(0)} = \mu_d$ as chemical potentials for visible and hidden sector fields, treating the system as a grand canonical ensemble. In order to conduct the thermodynamical analysis, we calculate the free energy of the system, to see which phase is thermodynamically preferable, for a fixed temperature. In the case of a hairless solution, we take into account the classical formula $F = E - TS - \mu Q - \mu_d Q_d$, where E is Brown-York quasilocal energy [4,5]. Nevertheless, this approach may cause problems in hairy solution analysis, being insufficient to capture the mass of the scalar field. Therefore, we treat this problem evaluating the on shell action in Euclidean signature $F = TS_{cl}$, which enables to take into considerations the nontrivial profile of scalar field constituting the solution of the underlying system of differential equations.

Solution of Eqs. (13)–(17) with $\psi = 0$ can be achieved analytically, giving the Reissner-Nordstrom (RN) dark matter black object [31]. To proceed further and accomplish the complete numerical analysis of the underlying equations, we implement the shooting method, integrating the aforementioned relations from r_h to r_b, using the fourth order Runge-Kutta method. From the set of free parameters, we fix the scalar magnitude on the event horizon ψ_0 and pick r_h, ϕ_1, and χ_1 to be shooting parameters. Moreover, we impose values on both chemical potentials that serve as constrains in our shooting procedure for ϕ_1 and χ_1. We set a domain of shooting parameters from the series expansion of the solutions near the horizon, then by using the iterative bisections one finds a solution that meets constrains, with a desired tolerance. Therefore, parameters $\{\mu_d, \alpha\}$, which are controlling, respectively, amount of *dark charge* and the coupling strength remain free; thus, they can be varied to see their impact on the system in question. For convenience, let us refer to the parameter $\psi^{(1)}$, as a *condensation*, which serves as a handy analogy to holographic theory. As mentioned above, in our numerical scheme, we treat μ_d as an input parameter in our code; however, one might not be interested in expressing these relations in a language of chemical potentials. Therefore, one might compute the total dark charge of the system

$$Q_d = \lim_{r \to r_b} \frac{1}{4\pi} \int_{\mathcal{S}^2} B_{\mu\nu} t^\mu n^\nu \sqrt{-g} d^2\theta, \tag{26}$$

where t_μ is a unit timelike vector and n_μ is a normal vector to the boundary. In the similar manner, we compute electrical charge for $F_{\mu\nu}$.

III. RESULTS

We commence with the hairy black hole solution (HBH), i.e., a system with an event horizon and nontrivial scalar field profile. The parameter space of HBH can be illustrated on a plane of chemical potential and Hawking temperature (μ-T) as a triangular shape. That region is bound between boson star phase from the left-hand side and generalized RN solution from the right-hand side. A schematic phase diagram has been presented in the Fig. 1, where both mentioned lines are marked. Moreover, the influence of the dark sector on phase boundaries is visualized by arrows, showing the trend of the flow by increasing the hidden sector chemical potential.

The hairy configuration can be achieved for a specific value of the chemical potential. Below the value μ_{RN} scalar cannot condensate and we get RN-dark matter black hole. On the other hand, for the value greater than the critical one, μ_c, the system becomes unstable. By stable hairy solution, we mean a constrained solution of the equations of motion (13)–(17) that fulfils the boundary conditions with desired tolerance and its free energy is lower than the free energy of RN and BS, making it the ground state of the system. We can define μ_c as the chemical potential for which the phase transition driven by temperature is no longer of second order and the condensate collapses. In the range between μ_{RN} and μ_c, we contend a typical second order phase transition, depicted in Fig. 2. In the vicinity of critical temperature, condensation can be described by a function $\psi^{(1)} \sim (T_c - T)^{1/2}$. It should also be noted that establishing an HBH solution requires relatively a large value of the scalar charge. In our calculation, we used $q = 100$ and a small mass of $m = 10^{-6}$.

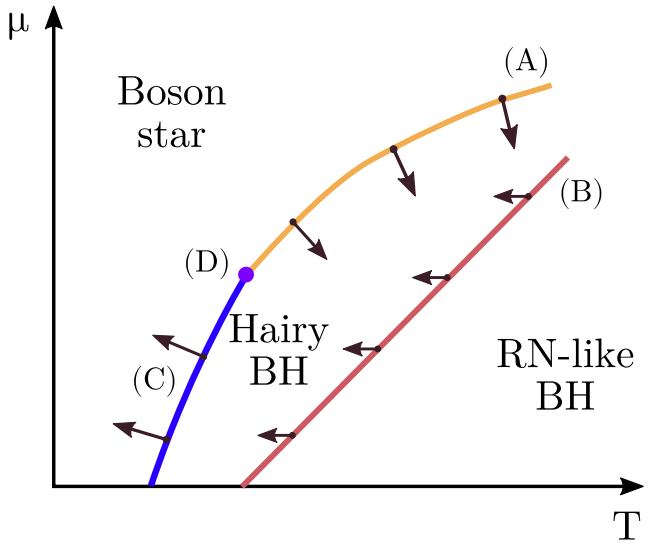

FIG. 1. A scheme of phase diagram of the described system. Blue-yellow line indicates the border between boson star and hairy black hole parameter space, while the red line depicts hairy BH—generalized RN BH phase boundary. The arrows on the scheme show us the flow of phase boundaries driven by the chemical potential of dark matter. Lines have been split and labeled from A to C, with a point D being the center of rotation of left-hand side boundary.

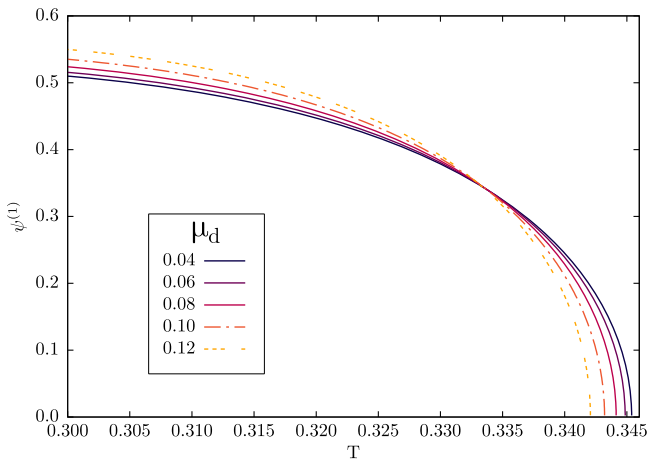

FIG. 2. Condensation $\psi^{(1)}$ as a function of temperature for the different values of μ_d and $\alpha = 10^{-3}$. For $\mu = 0.1$, a typical second order phase transition takes place, the dark matter presence influences the transition point and the condensation.

Let us now discuss physical mechanisms behind the phase boundaries flow from Fig. 1. When we cross the line of the critical chemical potential value μ_c, one encounters the *exotic phase*, where for one value of temperature we have two values of the condensation parameter $\psi^{(1)}$. Moreover, by evaluating its free energy, we can find it is so high that the hairy state is no longer stable—our

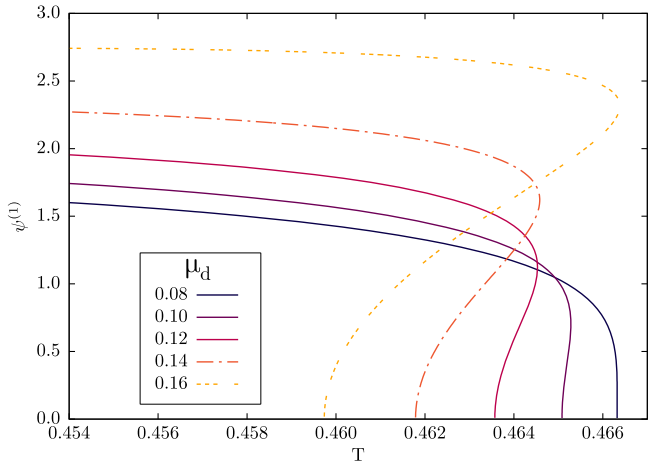

FIG. 3. Double valued profiles of condensation as functions of Hawking temperature caused by an increasing amount of dark matter in the system with $\alpha = 10^{-3}$ and $\mu = 0.14$. While the first transition for $\mu_d = 0.08$ might still be considered as a regular, the another strictly not—the value of condensation becomes double valued for some range of temperatures. Moreover, these solutions obey the boundary conditions but their free energy is larger than both BSs and RNs; therefore, they cannot be considered as thermodynamically preferred.

numerical method finds constrained solutions, but due to free energy leap, they are not thermodynamically preferred. The exotic phase effect occurs in case when scalar mass is close to or equal zero, for a mass away from this limit we do not obtain that phase. Instead, we have a sharp crossing, from stable solutions below μ_c to the situation when the equations of motion do not provide solutions with condensed scalar above the μ_c threshold at all. It is worth mentioning that a similar condensation-temperature profile has been shown in the so-called vector p-wave holographic superfluids [32], but a first order phase transition was hidden behind it. However, it was revealed that for the real value of the vector field, the model in question gave us the same description as holographic s-wave model with dark matter sector [33–34].

Dark matter gauge field plays an interesting role in this transition, as it accelerates the appearance, let us say, the exotic phase. For a larger value of dark sector chemical potential, $\psi^{(1)}$ becomes double valued for the lower chemical potential, which is depicted in Fig. 3, where μ_d has gradually increasing value. Moreover, when system enters the exotic phase, its free energy rises repeatedly and exceeds the free energy of RN black hole, so the hairy phase is no longer a preferred option. In this way, that effect restricts the range of chemical potential where the second order phase transition may occur, μ_c becomes a descending function of the dark charge [see curve (A) in the Fig. 1]. However, it cannot be increased without a limit. For every value of the electric charge, there exists a certain limit of dark charge, below which a formation of scalar hair is

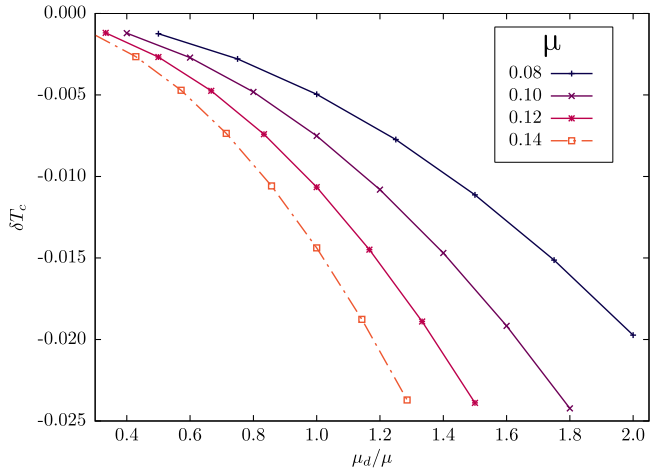

FIG. 4. Relative change of the critical temperature of hairy black hole—generalized RN black hole as a function of a ratio of chemical potentials. The temperature ratio has been normalized to the critical temperature of dark matter free solution, where $\mu_d = 0$.

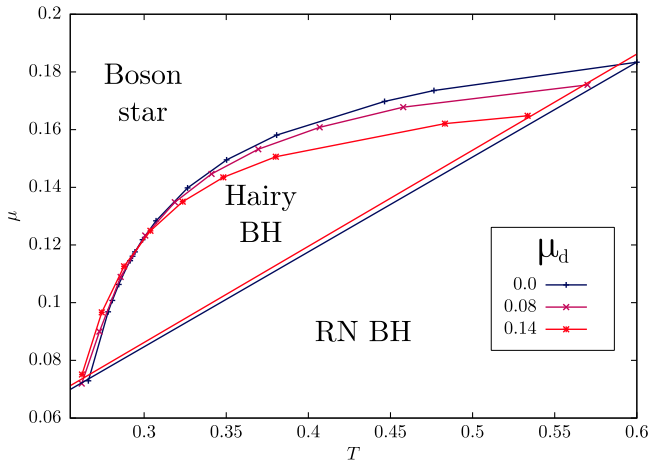

FIG. 5. Quasirotation of the phase transition boundary between boson star and hairy black hole caused by dark sector charge with α coupling equal to 10^{-4}. It can be observed that the μ threshold for hairy BH solution is significantly lowered and some parameter space of boson star is taken for the advantage of hairy BH for lower values of the chemical potential.

possible. Above it, such condensation cannot take place and no stable solutions are found. This phenomenon adds up both gravitational influence of the charge on the metric and nongravitational coupling between both gauge fields.

Now, let us draw our attention to the HBH-RN BH (B) border. An interesting effect that hidden sector exerts on the hairy black hole system is the shifting of the critical temperature of the phase transition. The larger growth of dark matter charge (and also μ_d) we observe, the lower value of the transition temperature one achieves. Such effect has been depicted in the Fig. 4, where the critical temperature ratio described by the relation

$$\delta T_c = \frac{T_c(\mu_d) - T_c(0)}{T_c(0)}$$

is shown as a function of the chemical potential of hidden sector normalized to the visible sector chemical potential. One can notice that the shift of the critical temperature is proportional to the square of μ_d. Obviously, it cannot decrease as low as one wishes and a certain limit exists which has been discussed in analytic solution of dark matter charged RN-like black hole [31]. The descent of the critical temperature becomes steeper for larger value of the chemical potential of the visible sector. It can be explained by the nongravitational interaction between fields via *kinetic mixing* term, which plays a significant role when both fields are sufficiently strong.

To proceed further, we shed some light on the influence of dark matter sector on the black hole-boson star phase transition in the stable area of small values of the chemical potential [line (C) in Fig. 1]. This process is depicted in Fig. 5, which asserts a phase diagram at the boundary between hairy black hole and boson star. While the boson star is a horizonless object, its Hawking temperature remains undefined. However, it is possible to calculate its characteristic—condensation and free energy as a function of chemical potential. Then to obtain the phase boundary curve, we start in the hairy black hole regime, then one moves toward lower Hawking temperatures and study the value of the free energy of the hairy black hole on the way. When it exceeds the free energy of a boson star, for the corresponding value of the chemical potential, the transition point is found. Both phases of the system are influenced by the hidden sector; nonetheless, the free energy of a boson star is affected much less than that of the black hole. Dark sector causes a significant drop of free energy of a hairy black hole. It means that the stability of a hairy solution is preserved for lower temperatures given the presence of the dark matter in the system. Such effect causes that hairy black hole solution is thermodynamically preferable for the lower Hawking temperatures and limits the emergence of boson star. The presence of α-coupling constant slightly diminishes the space of parameters for which boson star can emerge.

At last, it is sensible to mention some points that seem to be dark sector resistant. One of them appears on the phase boundary, labeled with (D) on the phase diagram scheme in Fig. 1. This point or rather its neighborhood does not seem to be susceptible on the dark charge presence in the system. For a particular numerical example, like in Fig. 5, it is placed around $\mu \approx 0.1160942$ and $T \approx 0.2929537$. Another one can be noticed in the condensation-Hawking temperature dependence presented in Fig. 2. All the curves

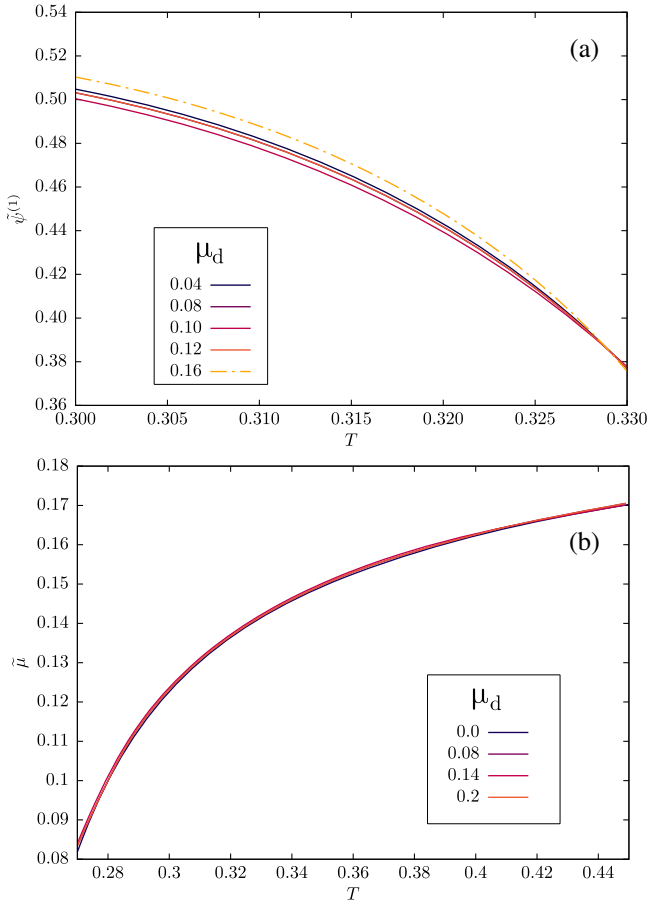

FIG. 6. Panel (a) presents condensation profile after the transformation performed in Eq. (29). The plot refers to the same data as in Fig. 2; however, it can be seen that the separation between curves is significantly smaller. In case of panel (b), which refers to Fig. 5, all curves appear to overlap with the dark matter free solution. The aforementioned transformation had removed the leading term of the dark sector influence.

certainly cross each other in one point, located at $\psi^{(1)} \approx 0.345$ and $T \approx 0.3325$. This interesting phenomenon shows that while the dark sector may modify the phase structure of the system and has an imprint on its critical quantities, there exists a specific configuration of the system, that remains completely untouched.

The points in question constitute the so-called *isosbestic* ones [35], where the curves dependent on temperature T and parametrized by values of dark matter chemical potential, intersect. They illustrate the influence of temperature on condensation $\psi^{(1)}$ and chemical potential of visible sector. At this point, we may perform a short analysis, which would reveal the leading order term of the dark sector influence. We take a following expansion of the condensate:

$$\psi^{(1)}(T,\mu_d) = \psi^{(1)}(T,0) + \mu_d^2\psi_1^{(1)}(T) + \mathcal{O}(\mu_d^3). \quad (27)$$

The second order term takes the approximated form

$$\psi_1^{(1)}(T) = \frac{\psi^{(1)}(T,\mu_{d1}) - \psi^{(1)}(T,\mu_{d2})}{\mu_{d1}^2 - \mu_{d2}^2}, \quad (28)$$

where in a certain example of curves from Fig. 2 we took $\mu_{d1} = 0.12$ and $\mu_{d2} = 0.08$. The zero of this function refers to the isosbestic point, where the contribution of μ_d is by definition none. By calculating the above function with help, the leading order of the influence of the dark sector may be subtracted from the main function

$$\tilde{\psi}^{(1)}(T,\mu_d) = \psi^{(1)}(T,\mu_d) - \mu_d^2\psi_1^{(1)}(T). \quad (29)$$

In the similar manner, we can expand and analyze the chemical potential as a function of Hawking temperature, parametrized by μ_d from boson star-hairy black hole phase boundary,

$$\mu(T,\mu_d) = \mu(T,0) + \mu_d^2\mu_1(T) + \mathcal{O}(\mu_d^3). \quad (30)$$

We define $\mu_1(T)$ analogically to (28) with $\mu_{d1} = 0.2$ and $\mu_{d2} = 0.08$ and perform the same transformation for $\mu(T,\mu_d)$ curve as for $\psi(T,\mu_d)$ in (29). The effect of these transformations is depicted in Fig. 6, where all curves tend to be much closer to each other than before. Obviously, the total effect of μ_d is not ruled out completely, since it is much more complex than in the considered expansion.

IV. CONCLUSION

In our paper, based on Einstein-Maxwell scalar dark matter theory, where the hidden sector is mimicked by the auxiliary $U(1)$-gauge field coupled to the ordinary Maxwell one by the kinetic mixing term with a coupling constant α, we elaborate two scenarios of emergence of a hairy black hole or a boson star. The main motivation standing behind our research was to shed some light on the influence of dark matter sector on the physics and thermodynamics of these systems.

The obtained results reveal that the coupling between visible and hidden sectors plays a complex role in the behavior of scalar hair. The parameter space (μ-T), where these solutions constitute a thermodynamically favorable phase, is being narrowed on two boundaries and extended to another one. The dark sector's presence strongly reduces the value of critical chemical potential, above which the hairy solution becomes unstable. Moreover, the critical temperature of HBH-RN-like solution is shifted toward the lower value of Hawking temperature. However, the boundary between HBH and boson stars is shifted toward the latter. The presence of the dark sector lowers the free energy of HBH system, which broadens the parameter space available for the emergence of the object in question by a noticeable extent, i.e., leaving boson star as an adverse phase in the low μ regime. It appears that the free energy of boson stars in the considered configuration reacts faintly to

the presence of $U(1)$-gauge dark matter field. While the response of the system is visible, it is much smaller in magnitude than of the condensate around a black hole. However, we suppose that interesting results may be achieved for more robust model of a scalar field, e.g., containing self-interacting terms.

In the view of presented results, it seems that the hairy solutions are not only battled by no-hair theorems originating from the theory of black holes, but also by a factor that is commonly present in our Universe—the dark matter. Even if such formation would be possible despite different obstacles a significant abundance of dark matter may prevent hairy solutions from emerging.

To visualize the impact of dark sector, we compute the area of HBH parameter space between both phase boundaries. One can consider simple integration $\int(\mu_{BS}(T) - \mu_{RN}(T))dT$ of the curves from Fig. 5, which reveals that the dark sector with $\mu_d = 0.14$ takes away approximately 27% of the hairy black hole's parameter space, compared to dark matter free solution. It is indeed a significant difference, because even if such formation would be possible despite different obstacles a significant abundance of dark sector may prevent hairy solutions from emerging.

The curves $\psi^{(1)}(T)$ and $\mu(T)$, parametrized by the values of dark matter chemical potential, reveal the isosbestic points, where they all intersect. One has the specific configurations of the considered system which is unaffected by the influence of hidden sector. At the points in question, we perform analysis revealing that the leading order influence of dark matter on the condensation $\psi^{(1)}$ and chemical potential of ordinary matter is quadratic in μ_d.

As a concluding remark, we present promising future research directions. We have elaborated the simple box-boundary models of a hairy black hole and a boson star (the so-called small boson star). The tantalizing question can be asked about the different boson star configurations with additional fields and potentials. Further investigations in this direction will be published elsewhere.

ACKNOWLEDGMENTS

We acknowledge K. I. Wysokinski and N. Sedlmayr for fruitful discussions on various occasions.

[1] R. Massey *et al.*, Dark matter maps reveal cosmic scaffolding, Nature (London) **445**, 286 (2007).
[2] J. P. Dietrich, N. Werner, D. Clowe, A. Finoguenov, T. Kitching, L. Miller, and A. Simionescu, A filament of dark matter between two cluster of galaxies, Nature (London) **487**, 202 (2012).
[3] G. Bertone and T. M. P. Tait, A new era in the search for dark matter, Nature (London) **562**, 51 (2018).
[4] J. W. York, Black-hole thermodynamics and the Euclidean Einstein action, Phys. Rev. D **33**, 2092 (1986).
[5] H. W. Braden, J. D. Brown, F. B. Whiting, and J. W. York, Charged black hole in a grand canonical ensemble, Phys. Rev. D **42**, 3376 (1990).
[6] G. W. Gibbons and M. J. Perry, Black Holes in Thermal Equilibrium, Phys. Rev. Lett. **36**, 985 (1976).
[7] S. A. Hartnoll, C. P. Herzog, and G. T. Horowitz, Building a Holographic Superconductor, Phys. Rev. Lett. **101**, 031601 (2008).
[8] Y. Peng, B. Wang, and Y. Liu, On the thermodynamics of the black hole and hairy black hole transitions in the asymptotically flat spacetime with a box, Eur. Phys. J. C **78**, 176 (2018).
[9] Y. Peng, Studies of a general flat space/boson star transition model in a box through a language similar to holographic superconductors, J. High Energy Phys. 07 (2017) 042.
[10] P. Basu, C. Krishnan, and P. N. Bala Subramanian, Hairy black holes in a box, J. High Energy Phys. 11 (2016) 041.
[11] P. Jetzer, Boson stars, Phys. Rep. **220**, 163 (1992); S. L. Libling and C. Palenzuela, Dynamical boson stars, Living Rev. Relativity **15**, 6 (2012).
[12] B. Kleihaus, J. Kunz, C. Lammerzahl, and M.List, Charged boson stars and black holes, Phys. Lett. B **675**, 102 (2009).
[13] B. Hartmann, B. Kleihaus, J. Kunz, and I. Schaffer, Compact boson stars, Phys. Lett. B **714**, 120 (2012).
[14] D. Pugliese, H. Quevedo, J. A. Rueda, and R. Ruffini, Charged boson stars, Phys. Rev. D **88**, 024053 (2013).
[15] S. Kumar, U. Kulshreshtha, D. S. Kulsreshtha, S. Kahlen, and J. Kunz, Some new results on charged compact boson stars, Phys. Lett. B **772**, 615 (2017).
[16] Y. Peng, Large regular reflecting stars have no scalar field hair, Eur. Phys. J. C **79**, 309 (2019).
[17] B. S. Acharya, S. A. R. Ellis, G. L. Kane, B. D. Nelson, and M. J. Perry, Lightest Visible-Sector Supersymmetric Particle is Likely Unstable, Phys. Rev. Lett. **117**, 181802 (2016).
[18] S. A. Abel and B. W. Schofield, Brane-antibrane kinetic mixing, millicharged particles and SUSY breaking, Nucl. Phys. **B685**, 150 (2004).
[19] S. A. Abel, J. Jaeckel, V. V. Khoze, and A. Ringwald, Illuminating the hidden sector of string theory by shining light through a magnetic field, Phys. Lett. B **666**, 66 (2008).
[20] S. A. Abel, M. D. Goodsell, J. Jaeckel, V. V. Khoze, and A. Ringwald, Kinetic mixing of the photon with hidden U(1)s in string phenomenology, J. High Energy Phys. 07 (2008) 124.
[21] D. Banerjee *et al.*, Search for Invisible Decays of Sub-GeV Dark Photons in Missing-Energy Events at the CERN SPS, Phys. Rev. Lett. **118**, 011802 (2017).
[22] P. Jean *et al.*, Early SPI/INTEGRAL measurements of 511 keV line emission from the 4th quadrant of the Galaxy, Astron. Astrophys. **407**, L55 (2003).

[23] J. Chang *et al.*, An excess of cosmic ray electrons at energies of 300–800 GeV, Nature (London) **456**, 362 (2008).
[24] O. Adriani *et al.* (PAMELA Collaboration), An anomalous positron abundance in cosmic rays with energies 1.5–100 Gev, Nature (London) **458**, 607 (2009).
[25] A. Geringer-Sameth and M. G. Walker, Indication of Gamma-Ray Emission from the Newly Discovered Dwarf Galaxy Reticulum II, Phys. Rev. Lett. **115**, 081101 (2015).
[26] K. K. Boddy and J. Kumar, Indirect detection of dark matter using MeV-range gamma-rays telescopes, Phys. Rev. D **92**, 023533 (2015).
[27] K. Van Tilburg, N. Leefer, L. Bougas, and D. Budker, Search for Ultralight Scalar Dark Matter with Atomic Spectroscopy, Phys. Rev. Lett. **115**, 011802 (2015).
[28] J. H. Chang, R. Essig, and S. D. McDermott, Revisiting Supernova 1987A constraints on dark photons, J. High Energy Phys. 01 (2017) 107.
[29] M. Crisler, R. Essig, J. Estrada, G. Fernandez, J. Tiffenberg, M. S. Haro, T. Volansky, and T.-T. Yu (SENSEI Collaboration), SENSEI: First Direct-Detection Constraints on Sub-GeV Dark Matter from a Surface Run, Phys. Rev. Lett. **121**, 061803 (2018).
[30] J. P. Lees *et al.*, Search for a Dark Photon in e^+e^- Collisions at BABAR, Phys. Rev. Lett. **113**, 201801 (2014).
[31] B. Kiczek and M. Rogatko, Ultra-compact spherically symmetric dark matter charged star objects, J. Cosmol. Astropart. Phys. 09 (2019) 049.
[32] R.-G. Cai, L. Li, and L.-F. Li, A holographic p-wave superconductor model, J. High Energy Phys. 01 (2014) 032.
[33] M. Rogatko and K. I. Wysokinski, P-wave holographic superconductor/insulator phase transitions affected by dark matter sector, J. High Energy Phys. 03 (2016) 215.
[34] M. Rogatko and K. I. Wysokinski, Condensate flow in holographic models in the presence of dark matter, J. High Energy Phys. 10 (2016) 152.
[35] D. Vollhardt, Characteristic Crossing Points in Specific Heat Curves of Correlated Systems, Phys. Rev. Lett. **78**, 1307 (1997); S. Uchida, T. Ido, H. Takagi, T. Arima, Y. Tokura, and S. Tajima, Optical spectra of $La_{2-x}Sr_xCuO_4$: Effect of carrier doping on the electronic structure of the CuO_2 plane, Phys. Rev. B **43**, 7942 (1991); J. K. Freericks, T. P. Devereaux, and R. Bulla, Exact theory for electronic Raman scattering of correlated materials in infinite dimensions, Phys. Rev. B **64**, 233114 (2001).